Cofilin under control of β-arrestin-2 in NMDA-dependent dendritic spine plasticity, long-term depression (LTD), and learning

Crystal G. Pontrello[a,b], Min-Yu Sun[c], Alice Lin[a], Todd A. Fiacco[b,c], Kathryn A. DeFea[a], and Iryna M. Ethell[a,b,c,1]

[a]Division of Biomedical Sciences, [b]Neuroscience Graduate Program, and [c]Cell, Molecular, and Developmental Biology Graduate Program, University of California, Riverside, CA 92521

Dendritic spines are dynamic, actin-rich structures that form the postsynaptic sites of most excitatory synapses in the brain. The F-actin severing protein cofilin has been implicated in the remodeling of dendritic spines and synapses under normal and pathological conditions, by yet unknown mechanisms. Here we report that β-arrestin-2 plays an important role in NMDA-induced remodeling of dendritic spines and synapses via translocation of active cofilin to dendritic spines. NMDAR activation triggers cofilin activation through calcineurin and phosphatidylinositol 3-kinase (PI3K)-mediated dephosphorylation and promotes cofilin translocation to dendritic spines that is mediated by β-arrestin-2. Hippocampal neurons lacking β-arrestin-2 develop mature spines that fail to remodel in response to NMDA. β-Arrestin-2–deficient mice exhibit normal hippocampal long-term potentiation, but significantly impaired NMDA-dependent long-term depression and spatial learning deficits. Moreover, β-arrestin-2–deficient hippocampal neurons are resistant to Aβ-induced dendritic spine loss. Our studies demonstrate unique functions of β-arrestin-2 in NMDAR-mediated dendritic spine and synapse plasticity through spatial control over cofilin activation.

T he postsynaptic sites of the majority of excitatory synapses in the central nervous system are found on dynamic protrusions called dendritic spines (1–5). Dendritic spines are filamentous actin (F-actin)–rich structures, which are regulated by actin-binding proteins that sever, bundle, polymerize, or cap F-actin filaments (6). Structural plasticity of dendritic spines has been linked to synaptic plasticity (7, 8) and is thought to underlie learning and memory processes (9), whereas defects in dendritic spine morphology are associated with certain neurological disorders (10, 11). Cofilin is an F-actin–severing protein that increases the turnover of F-actin by severing the filaments and creating new barbed ends for F-actin growth (12–17). Several studies suggest that cofilin activation by dephosphorylation may trigger dendritic spine remodeling in neurons, resulting in the destabilization and transformation of mature mushroom-shaped spines with large heads into immature thin spines in hippocampal neurons (18, 19). Moreover, cofilin-mediated plasticity was reported to underlie both dendritic spine enlargement and stabilization induced by long-term potentiation (LTP) (20), as well as spine shrinkage and elimination associated with long-term depression (LTD) (21). Recent studies showing an increased number of mature spines with large heads in cofilin-deficient neurons support the role of cofilin in dendritic spine plasticity (22). Excessive cofilin activity has been implicated in stress-induced cofilin–actin rods that are found in the brain with several neurological disorders associated with dendritic spine loss (23, 24). Conversely, the suppression of endogenous cofilin activation by phospho-mimetic cofilin[S3D] has been reported to protect neurons against amyloid-beta (Aβ)-mediated spine loss (25, 26). Therefore, understanding cofilin regulation in dendritic spines will advance our knowledge of normal learning and memory processes, as well as neuropathology such as that found in Alzheimer's disease.

Whereas cofilin activation is regulated through its dephosphorylation, the mechanisms that achieve temporal and spatial control over cofilin activity in dendritic spines have not been identified. β-Arrestins are known to be involved in the desensitization and internalization of G-protein–coupled receptors (27–29) and are also recognized for their ability to regulate F-actin organization and cytoskeletal dynamics through the scaffolding of actin assembly proteins (30–32). Here we demonstrate that β-arrestin-2 spatially regulates cofilin localization in dendritic spines and plays an important role in NMDA-induced dendritic spine and synapse remodeling. NMDA-induced structural plasticity depends on the translocation of active cofilin into dendritic spines, which is regulated by the scaffolding protein β-arrestin-2. Our studies show that NMDA-induced translocation of a constitutively active cofilin mutant into dendritic spines is disrupted in β-arrestin-2 KO neurons. β-Arrestin-2 KO neurons develop normal mature spines both in vitro and in vivo, but these spines fail to remodel in response to NMDA or overexpression of constitutively active cofilin[S3A], possibly due to abnormal spatial regulation of cofilin in neurons lacking β-arrestin-2. We also find functional abnormalities, as β-arrestin-2 KO mice exhibit impaired hippocampal LTD and spatial learning deficits in the radial arm water maze. Furthermore, β-arrestin-2–deficient hippocampal neurons are resistant to a pathological form of spine plasticity, Aβ-induced dendritic spine loss. Our studies demonstrate that β-arrestin-2 regulates both physiological and pathological forms of dendritic spine and synapse plasticity through spatial control over cofilin activation in dendritic spines.

Results

NMDA-Mediated Remodeling of Mature Dendritic Spines and Synapses Is Blocked by Phospho-Mimetic Cofilin[S3D]. Our previous studies have shown that activation of the NMDA receptor promotes dendritic spine remodeling in cultured hippocampal neurons (18). To determine whether cofilin underlies this event, we induced NMDA-dependent chemical LTD in cultured hippocampal neurons expressing control GFP, wild-type (WT) cofilin, constitutively active cofilin[S3A], or phospho-mimetic cofilin[S3D]. Control hippocampal neurons exhibited a high occurrence of mature mushroom-shaped dendritic spines with large heads and short necks, resulting in a high spine head area-to-length ratio (Fig. 1). The mature spines were associated with synaptophysin-positive puncta, demonstrating the proximity of
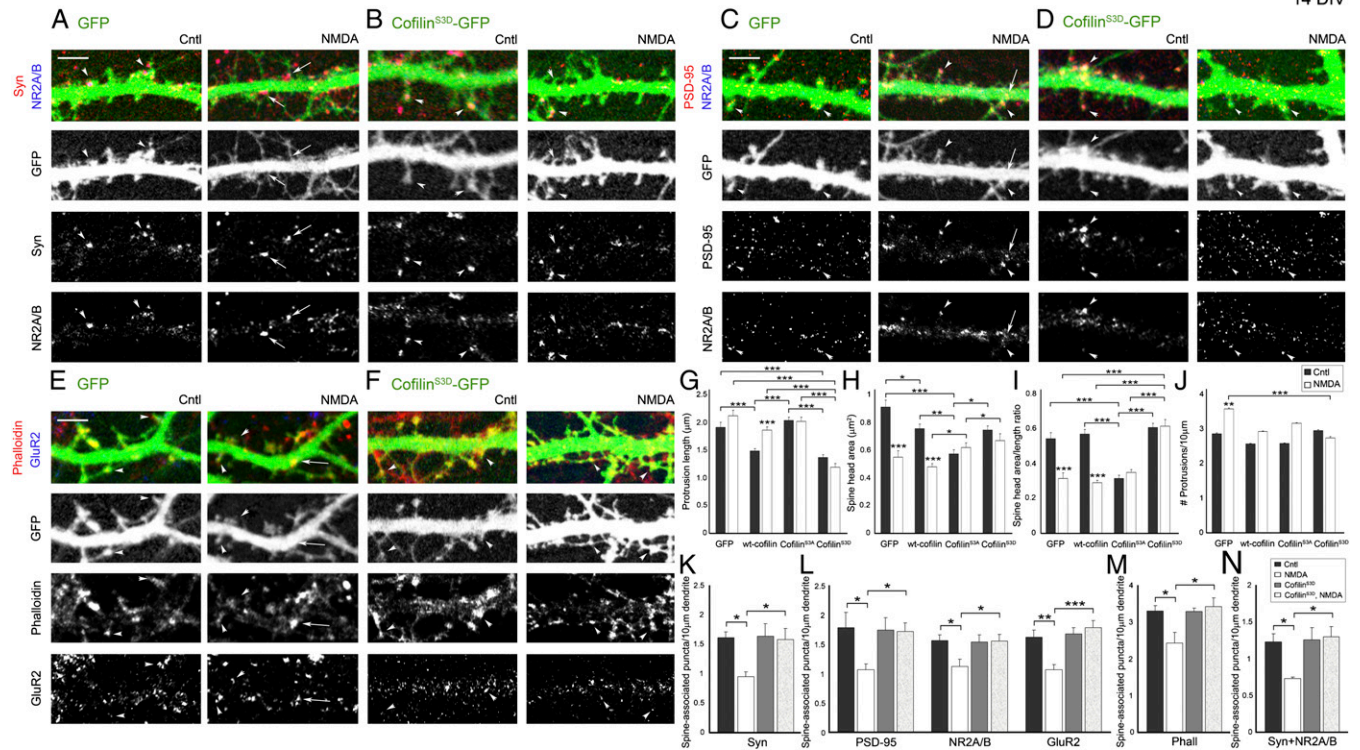
Fig. 1. NMDA-mediated remodeling of mature dendritic spines and synapses is blocked by phospho-mimetic cofilin[S3D]. (*A–F*) Confocal images showing the dendrites of 14 days in vitro (DIV) hippocampal neurons expressing GFP (*A*, *C*, and *E*) or GFP-tagged cofilin[S3D] (cofilin[S3D]-GFP; *B*, *D*, and *F*). Neurons were untreated (Cntl), or treated with 50 μM NMDA in Mg²⁺-free solution for 5 min to activate NMDA receptors, followed by NMDA washout and 60 min incubation in conditioned media (NMDA). Pre- and postsynaptic sites were identified by immunostaining against synaptophysin (Syn, *A* and *B*), PSD-95 (*C* and *D*), the NMDAR subunits NR2A/B (*A–D*), and the AMPAR subunit GluR2 (*E* and *F*). F-actin was detected by rhodamine-coupled phalloidin (*E* and *F*). Arrowheads denote positive puncta that are associated with dendritic spines, and arrows denote positive puncta in the dendritic shaft. (Scale bars, 10 μm.) (*G–J*) Quantitative analysis of spine length (*G*), head area (*H*), head area/length ratio (*I*), and density (*J*) in untreated (Cntl) and NMDA-treated (NMDA) neurons expressing GFP, WT cofilin, constitutively active cofilin[S3A], or phospho-mimetic cofilin[S3D]. Histograms show mean ± SEM (n = 100–200 spines from 7–10 neurons per condition). Statistical analysis was performed using one-way ANOVA followed by Tukey's multiple-comparison posttest (*P < 0.05, **P < 0.01, ***P < 0.001). (*K–N*) Quantitative analysis of the numbers of synaptophysin (Syn-), PSD-95–, NR2A/B–, GluR2-, and Phalloidin (Phall)-positive puncta associated with dendritic spines per 10 μm of dendrite in untreated (Cntl) or NMDA-treated (NMDA) neurons expressing GFP or cofilin[S3D]. Histograms show mean ± SEM (n = 7–10 neurons per condition). Statistical analysis was performed using one-way ANOVA followed by Tukey's multiple-comparison posttest (*P < 0.05, **P < 0.01, ***P < 0.001).

presynaptic boutons, and contained the postsynaptic density (PSD) protein PSD-95, as well as the NR2A/B and GluR2 subunits of NMDARs and AMPARs, respectively (Fig. 1 *A–F*). NMDAR activation increased the proportion of immature dendritic spines, indicated by a decrease in spine head size and the spine head area-to-length ratio (Fig. 1 *H* and *I*), and induced growth of new filopodia resulting in an overall increase in protrusion density (Fig. 1*J*). NMDAR activation also led to a decrease in the numbers of synaptophysin, PSD-95, NR2A/B, and GluR2 puncta that were associated with dendritic spine heads, which could be a result of spine head shrinkage (Fig. 1 *K–N*). There was a subsequent increase in synaptic puncta along the dendritic shaft with no change in the overall number of these pre- and postsynaptic puncta following NMDAR activation, suggesting their redistribution from the spine heads to the dendritic shaft rather than their elimination.

NMDA-induced changes in dendritic spine morphology and the number of synaptic sites associated with dendritic spines were dependent on cofilin activation, as its inhibition by overexpression of phospho-mimetic cofilin[S3D] blocked NMDA-induced shrinkage of dendritic spine heads and prevented subsequent loss of synaptic proteins from dendritic spines (Fig. 1 *K–N*). In contrast, overexpression of constitutively active cofilin[S3A] induced dendritic spine head shrinkage, similar to the effects of NMDA treatment. NMDAR activation did not induce

further spine head shrinkage in neurons expressing cofilin[S3A], perhaps because these spines already exhibit smaller heads before NMDA treatment (Fig. 1 *G–J*). Our results suggest that NMDA may induce remodeling of dendritic spines and synapses through the regulation of cofilin activation in dendritic spines.

NMDAR Activation Promotes Rapid Translocation of Active Cofilin to Dendritic Spines, Which Is Disrupted in β-Arrestin-2 KO Neurons. We found that in addition to cofilin dephosphorylation, proper localization of active cofilin is essential for its effects on dendritic spines and synapses. Our studies indicate that acute NMDA treatment of 14 days in vitro (DIV) hippocampal neurons results in a rapid translocation of both WT cofilin and the nonphosphorylatable constitutively active cofilin[S3A] (Movie S1), but not the phospho-mimetic cofilin[S3D] mutant, to the heads of dendritic spines within 5 min of NMDA treatment (Fig. 2). In addition, cofilin[S3A] is diffusely distributed throughout the spines and dendritic shaft before NMDA treatment, indicating that dephosphorylation alone is not sufficient to trigger cofilin clustering in dendritic spines.

The scaffolding proteins β-arrestins, which were recently suggested to regulate cofilin localization in migrating cells (33, 34), were prime candidates for the regulation of cofilin translocation in response to NMDAR activation. First, we examined the effects of NMDA on the localization of WT cofilin, constitutively active cofilin[S3A], or inactive phospho-mimetic cofilin[S3D] in
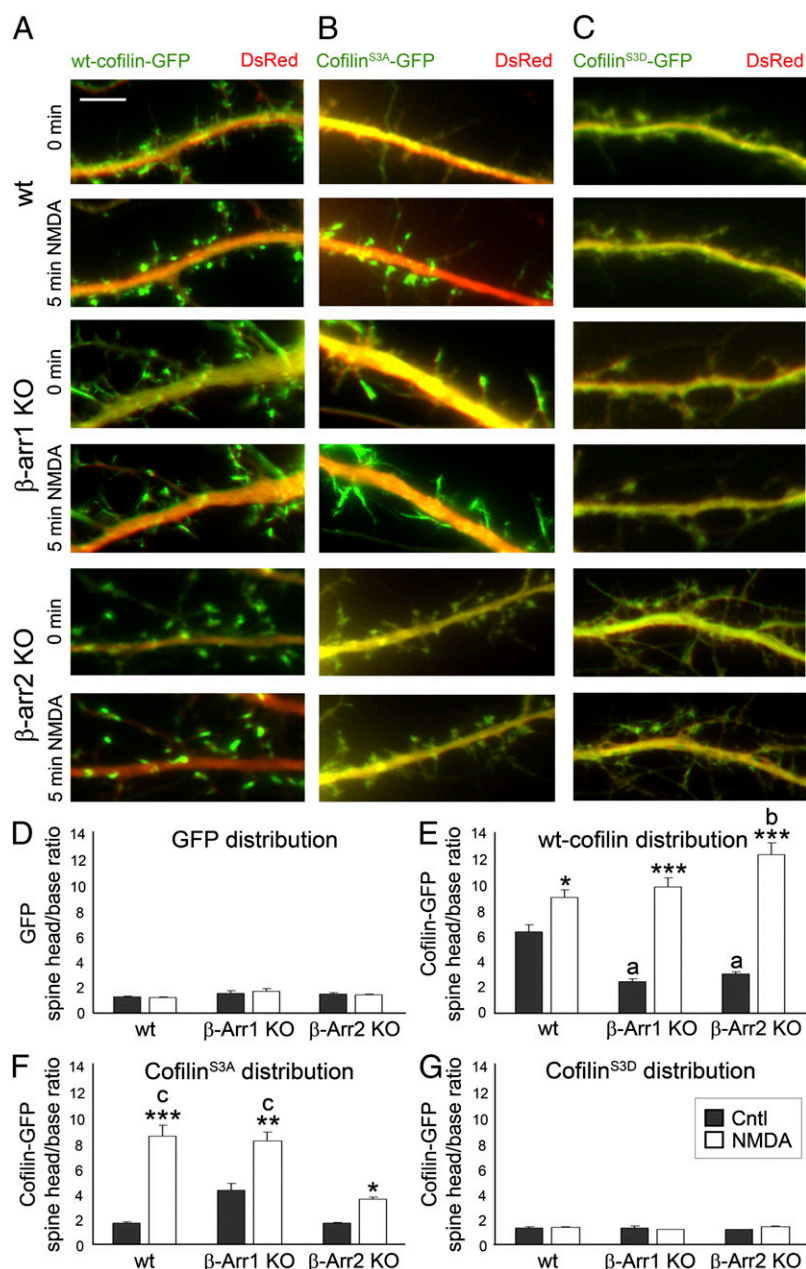
Fig. 2. NMDAR activation promotes rapid translocation of cofilin to dendritic spines, which is disrupted in β-arrestin-2 KO neurons. (*A–C*) Time-lapse fluorescent images showing the dendrites of WT, β-arrestin-1 KO, or β-arrestin-2 KO hippocampal neurons at 14 DIV expressing DsRed (red) and WT cofilin-GFP (*A*), cofilin^{S3A}-GFP (*B*), or cofilin^{S3D}-GFP (*C*), before (Cntl) or 5 min after treatment with NMDA. (Scale bars, 10 μm.) See also Movies S1 and S2. (*D–G*) Quantitative analysis of the distribution of GFP and GFP-tagged cofilin before and after NMDA treatment is shown by the dendritic spine head-to-base (head/base) ratio of GFP fluorescence, normalized against DsRed fluorescence. A ratio of 1 would indicate uniform distribution of GFP or GFP-tagged cofilin in the spine heads and dendritic shaft (base), whereas a ratio that is significantly >1 would indicate specific targeting of GFP-tagged cofilin to dendritic spines. Histograms show mean ± SEM (*n* = 100–200 spines from five neurons per condition). Statistical analysis was performed using one-way ANOVA followed by Tukey's multiple-comparison posttest. *$P < 0.05$, **$P < 0.01$, ***$P < 0.001$ compared with respective control; *a* indicates value significantly different from that of untreated WT neurons ($P < 0.001$); *b* indicates value significantly different from that of NMDA-treated WT neurons ($P < 0.01$); *c* indicates value significantly different from that of NMDA-treated β-arrestin-2 KO neurons ($P < 0.001$).

β-arrestin-1 KO and β-arrestin-2 KO hippocampal neurons (Fig. 2). NMDA-triggered translocation of constitutively active cofilin^{S3A} into the spines was seen in WT hippocampal neurons (Fig. 2 *B* and *F* and Movie S1), but was impaired in β-arrestin-2 KO neurons (Fig. 2 *B* and *F* and Movie S2). This reduction in the level of cofilin clustering in spines following NMDA treatment demonstrates that β-arrestin-2 is required for proper translocation of active nonphosphorylatable cofilin^{S3A} to the spines in response to NMDAR activation. In contrast to active non-phosphorylatable cofilin^{S3A}, NMDA-induced translocation of WT cofilin to dendritic spines was not affected in either β-arrestin-1 KO or β-arrestin-2 KO neurons (Fig. 2 *A* and *E*). It is possible that β-arrestin-1 may regulate cofilin translocation in β-arrestin-2 KO neurons, which is blocked by the substitution of Ser to Ala in active nonphosphorylatable cofilin^{S3A}, whereas β-arrestin-2 controls translocation of active nonphosphorylatable cofilin^{S3A} in β-arrestin-1 KO neurons. These results suggest that both β-arrestins may be involved in the translocation of cofilin,
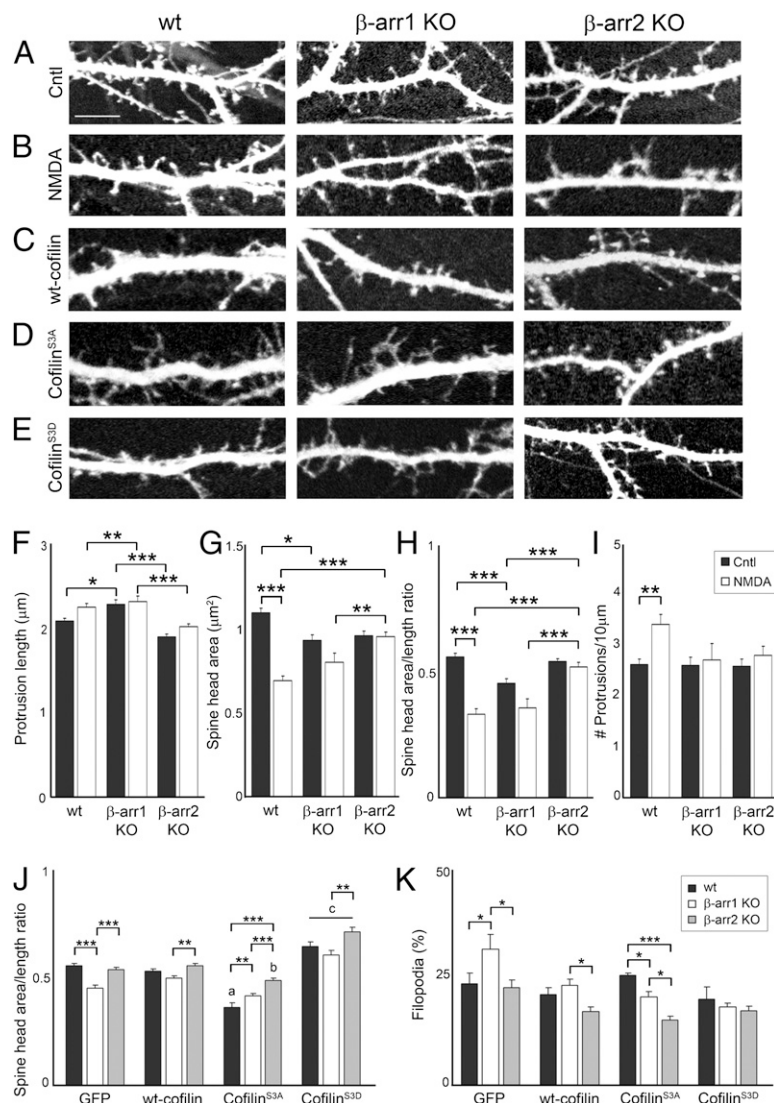
Fig. 3. β-Arrestin-2 KO neurons develop normal mature spines that are resistant to spine remodeling induced by NMDA or constitutively active cofilin^{S3A}. (*A–E*) Confocal images showing the dendrites of 14 DIV hippocampal neurons from WT, β-arrestin-1 KO, or β-arrestin-2 KO hippocampal neurons expressing DsRed and GFP (*A* and *B*) or DsRed and WT cofilin-GFP (*C*), cofilin^{S3A}-GFP (*D*), or cofilin^{S3D}-GFP (*E*). (*B*) Neurons were treated with NMDA (50 μM, 5 min), followed by washout and incubation in conditioned media for 60 min. (Scale bar, 10 μm.) (*F–K*) Quantitative analysis of spine length (*F*), head area (*G*), head area/length ratio (*H* and *J*), density (*I*), and percentage of filopodia (*K*). Graphs display mean ± SEM (*n* = 600–800 spines from 12–15 neurons per condition). Statistical analysis was performed using one-way ANOVA followed by Tukey's multiple-comparison posttest. *$P < 0.05$, **$P < 0.01$, ***$P < 0.001$; *a* indicates value significantly different from that of WT neurons expressing GFP, WT cofilin, or cofilin^{S3D} ($P < 0.001$); *b* indicates value significantly different from that of β-arrestin-2 KO neurons expressing GFP ($P < 0.05$), WT cofilin ($P < 0.01$), or cofilin^{S3D} ($P < 0.001$); *c* indicates value significantly different from those of all other conditions of the corresponding genotype ($P < 0.001$).

but β-arrestin-2 is necessary for the translocation of the active form of cofilin to the spines in response to NMDAR activation.

β-Arrestin-2 KO Neurons Are Resistant to NMDA-Induced Dendritic Spine Remodeling. The NMDA-induced translocation of cofilin to spines, which occurred rapidly within 5 min of NMDA treatment, is followed by transformation of mature spines with large heads into immature thin spines with small heads (Fig. S1). To investigate whether the ability of β-arrestin-2 to localize active cofilin into dendritic spines is required for NMDA-induced spine remodeling, we examined the effects of NMDA on spine morphology in hippocampal neurons that lack β-arrestin-1 or β-arrestin-2. Our results indicate that deletion of the scaffolding protein β-arrestin-2 abolished the ability of NMDA to induce dendritic spine remodeling. Whereas NMDA treatment of WT neurons resulted in a more immature spine phenotype, the morphology of β-arrestin-2 KO neurons did not change with

NMDA treatment (Fig. 3 *A*, *B*, and *F–I*). Statistical analysis showed no significant changes in spine length, spine head area, and the spine head area-to-length ratio in NMDA-treated β-arrestin-2 KO neurons compared with untreated β-arrestin-2 KO neurons (Fig. 3 *F–H*). Although the deletion of β-arrestin-2 blocked NMDA-induced spine remodeling, it did not affect normal development of dendritic spines, as β-arrestin-2 KO neurons developed mature spines with large heads that were similar to WT neurons in 14 DIV hippocampal cultures (Fig. 3 *A*, *B*, and *F–J*). In contrast, β-arrestin-1 KO neurons exhibited more immature spines that were longer with smaller heads and lower spine head area-to-length ratios than WT neurons, but phospho-mimetic cofilin^{S3D} rescued a mature spine phenotype in the β-arrestin-1 KO neurons (Fig. 3 *E* and *J*). This result suggests that β-arrestin-1 is required for normal dendritic spine development and may act to suppress excessive cofilin activity in dendritic spines, resulting in spine maturation, whereas

loss of β-arrestin-1 may increase the vulnerability of β-arrestin-1 KO neurons to pathological conditions. Indeed, the overexpression of active nonphosphorylatable cofilin[S3A] in β-arrestin-1 KO neurons resulted in the formation of structures resembling cofilin–actin rods (Fig. 2B) that have been reported in conditions of cellular stress (35, 36). These results suggest that both the ability of β-arrestin-2 to control NMDA-induced spine remodeling and the β-arrestin-1–dependent development of mature spines depend on cofilin activation.

β-Arrestin-2 Deletion Affects Dendritic Spine Remodeling Induced by Constitutively Active Cofilin[S3A].

If the ability of β-arrestin-2 to regulate the localization of cofilin in dendritic spines underlies NMDA-mediated spine remodeling, then deletion of β-arrestin-2 might also affect dendritic spine remodeling induced by constitutively active cofilin[S3A]. Indeed, constitutively active cofilin[S3A] failed to cluster in dendritic spines of β-arrestin-2–deficient neurons in response to NMDA treatment (Fig. 2B), and the ability of constitutively active cofilin[S3A] to induce dendritic spine remodeling was also disrupted in β-arrestin-2–deficient neurons (Fig. 3D). Whereas constitutively active cofilin[S3A] induced an immature spine phenotype in WT hippocampal neurons, similar to the effects of NMDA treatment, β-arrestin-2 KO neurons expressing constitutively active cofilin[S3A] exhibited mature spines with a larger head area-to-length ratio and lower percentage of immature filopodia-like protrusions than either WT neurons expressing constitutively active cofilin[S3A] or β-arrestin-1 KO neurons (Fig. 3 D, J, and K). Our results suggest that β-arrestin-2 plays an important role in the translocation of active cofilin to dendritic spines to regulate spine remodeling in response to NMDA.

Overexpression of β-Arrestin-1 or β-Arrestin-2 Reverses the Effect of β-Arrestin Deletion on Dendritic Spine Morphology Under Normal Synaptic Activity or in Response to NMDA.

We were able to reverse the effects of β-arrestin-1 KO on dendritic spine morphology by overexpressing β-arrestin-1 that was tagged with the FLAG peptide sequence (DYKDDDDK) in β-arrestin-1–deficient neurons (Fig. 4 A, C, and E). Analysis of the distribution of transfected FLAG-tagged β-arrestin-1 revealed diffuse localization throughout both the dendritic shafts and spines (Fig. 4 C and F). In addition, overexpression of FLAG-tagged β-arrestin-2 rescued NMDA-induced spine remodeling in β-arrestin-2–deficient

neurons (Fig. 4 B, D, and E), confirming that β-arrestin-2 is involved in NMDA-mediated dendritic spine remodeling.

We also found that β-arrestin-2 can directly interact with WT cofilin, cofilin[S3A], and cofilin[S3D], with the highest affinity toward constitutively active cofilin[S3A] (Fig. 4G). These findings are consistent with a model in which β-arrestin-2 binds to activated cofilin and promotes its translocation to dendritic spines. β-Arrestin-2 is also distributed equally among dendritic spines and shafts, but appears to form clusters in response to NMDA treatment, which are detected in the heads of dendritic spines (Fig. 4 D and F). These results suggest that both β-arrestins are involved in spine development and maintenance under normal synaptic activity, whereas β-arrestin-2 is also involved in cofilin-mediated dendritic spine remodeling in response to NMDA.

β-Arrestin-2 Mediates NMDA-Induced Cofilin Translocation Independent of Cofilin Dephosphorylation.

β-Arrestins may also regulate cofilin phosphorylation levels through scaffolding cofilin with its kinase LIM kinase 1 (LIMK1, where LIM is an acronym of the three gene products Lin-11, Isl-1, and Mec-3)-1 or phosphatase chronophin (CIN) (33, 34), so we examined whether NMDA-induced cofilin dephosphorylation is affected in β-arrestin-2 KO neurons. Whereas deletion of β-arrestin-2 affected NMDA-induced translocation of active cofilin to dendritic spines and spine remodeling, it was not sufficient to block NMDA-mediated cofilin dephosphorylation, as we observed reduced levels of phosphorylated cofilin in NMDA-treated β-arrestin-2 KO neurons compared with untreated controls (Fig. 5 A and B). Similar to previously published reports, we found that NMDA-induced activation of calcineurin and a Ras-PI3K pathway is responsible for NMDA-mediated cofilin dephosphorylation (37, 38), as concurrent treatment of hippocampal neurons with a calcineurin inhibitor [50 µM cyclosporin A (CycA)] and a PI3K inhibitor [50 µM LY294,002 (LY)] completely blocked NMDA-induced cofilin dephosphorylation in hippocampal neurons (Fig. 5 A and B). However, dephosphorylation is not required for cofilin clustering in dendritic spines following NMDAR activation, as inhibition of cofilin dephosphorylation did not prevent NMDA-induced translocation of WT cofilin to dendritic spines, an effect that was blocked by the specific NMDAR inhibitor MK801 (Fig. 5 C and F). Nevertheless, inhibition of cofilin dephosphorylation with the calcineurin and PI3K inhibitors did block NMDA-induced changes in dendritic spine morphology, suggesting that cofilin can
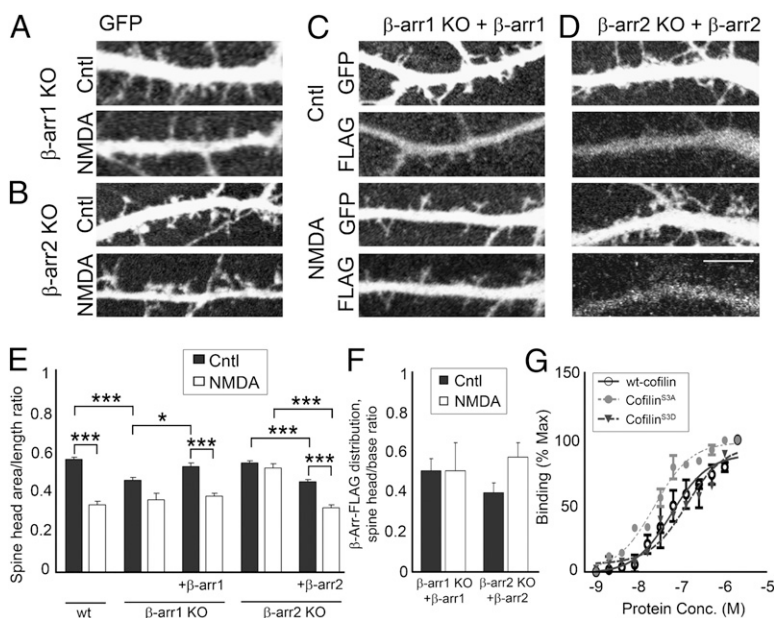

Fig. 4. Overexpression of β-arrestin-1 or β-arrestin-2 reverses the effect of β-arrestin deletion on dendritic spine morphology under normal synaptic activity or in response to NMDA. (A–D) Confocal images showing the dendrites of 14 DIV hippocampal neurons from β-arrestin-1 KO or β-arrestin-2 KO mice expressing GFP alone (A and B) or GFP with FLAG-tagged β-arrestin-1 (C) or FLAG-tagged β-arrestin-2 (D). (Scale bar, 10 µm.) (E and F) Quantitative analysis of dendritic spine morphology (spine head area/length ratio, E) and the distribution of FLAG-tagged β-arrestins (F). The ratio of β-arrestin immunoreactivity was measured in the spine head vs. the dendritic shaft (spine head/base ratio), in WT or KO neurons expressing FLAG-tagged β-arrestin-1 or -2. FLAG-tagged β-arrestin-1 or -2 was detected by immunostaining against FLAG and levels were normalized to GFP fluorescence. Graphs display mean ± SEM (n = 600 spines from 10 cells per condition). Statistical analysis was performed using one-way ANOVA followed by Tukey's multiple-comparison posttest (*P < 0.05, ***P < 0.001). (G) Mean binding of GST-tagged β-arrestin-2 was determined for WT cofilin, cofilin[S3A], and cofilin[S3D]. Integrated intensity from replicate experiments (n = 3) was determined and normalized to maximal signal. Curves were fit using a nonlinear regression dose–response model.
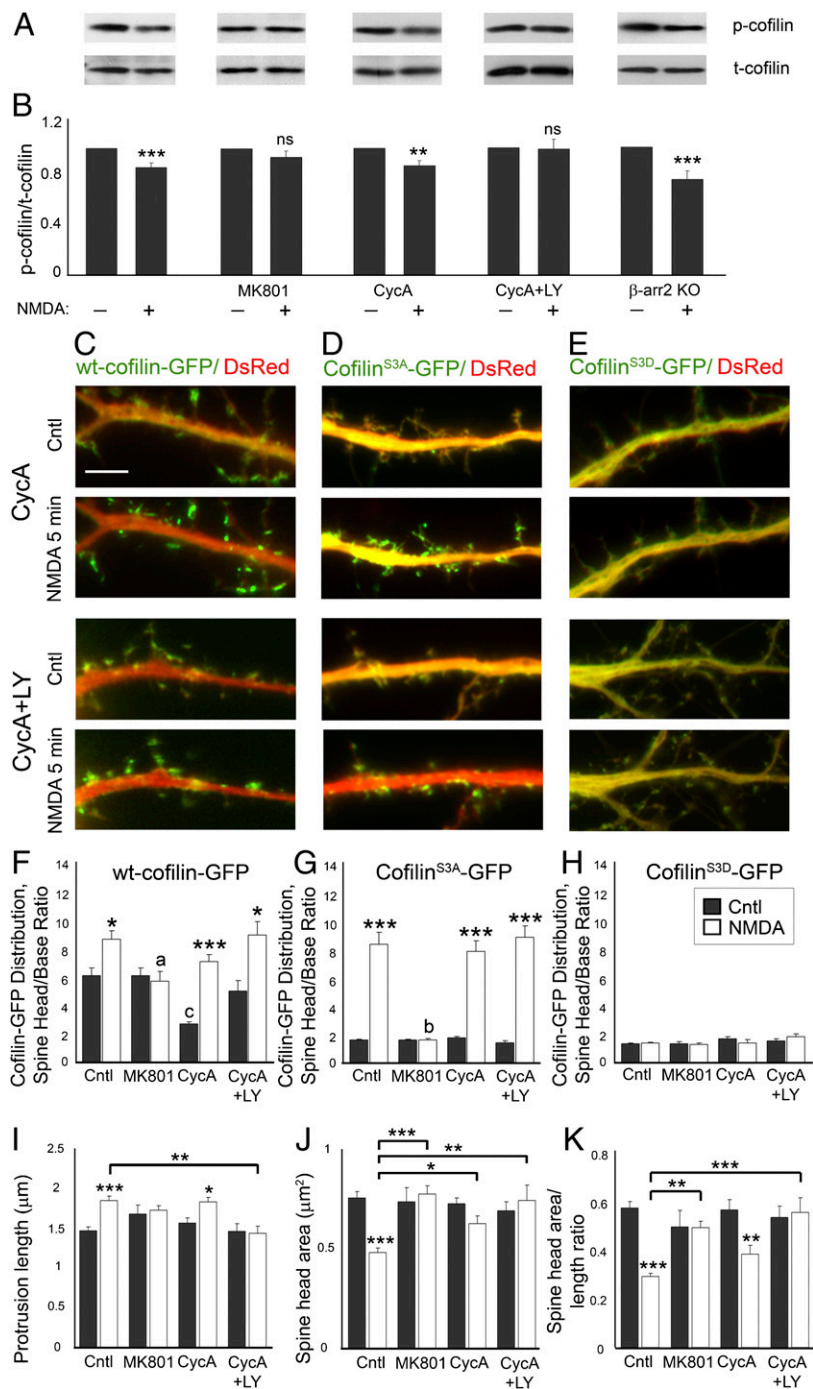
Fig. 5. Cofilin dephosphorylation is not required for cofilin translocation to dendritic spines, but is necessary for dendritic spine remodeling. (*A* and *B*) Fourteen DIV hippocampal neurons were treated with 50 μM NMDA in Mg^{2+}-free solution to activate NMDA receptors for 5 min with or without MK801 (10 μM), cyclosporin A (CycA, 50 μM), or LY294,002 (LY, 50 μM). Cell lysates were subjected to immunoblotting with anti–phospho-cofilin antibodies. The blots were stripped and reprobed against total cofilin. The levels of phospho-cofilin were quantified by densitometry and normalized to total cofilin levels, respectively. Experimental values represent mean ± SEM (*n* = 5–10). Statistical analysis was performed using Student's *t* test (**$P < 0.01$, ***$P < 0.001$). (*C–E*) Time-lapse fluorescent images showing the dendrites of 14 DIV WT hippocampal neurons expressing DsRed (red) and WT cofilin-GFP (*C*), cofilin^{S3A}-GFP (*D*), or cofilin^{S3D}-GFP (*E*), before (Cntl) or 5 min after treatment with NMDA. (Scale bars, 10 μm.) (*F–H*) Quantitative analysis of the distribution of GFP-tagged cofilin in neurons expressing WT cofilin-GFP (*F*), cofilin^{S3A}-GFP (*G*), or cofilin^{S3D}-GFP (*H*), before and after NMDA treatment, with and without MK801, CycA, or CycA and LY294,002 (CycA+LY). The dendritic spine head-to-base (head/base) ratio of GFP fluorescence is normalized against DsRed fluorescence. Histograms show mean ± SEM (*n* = 100–200 spines from 5 neurons per condition). Statistical analysis was performed using one-way ANOVA followed by Tukey's multiple-comparison posttest. *$P < 0.05$, ***$P < 0.001$ compared with respective control; *a* and *b* indicate values significantly different from those of NMDA-treated neurons without inhibitors (*a*, $P < 0.05$; *b*, $P < 0.001$); *c* indicates value significantly different from that of untreated neurons (*c*, $P < 0.01$). (*I–K*) Quantitative analysis of spine length (*I*), head area (*J*), and head area/length ratio (*K*) in WT hippocampal neurons expressing WT cofilin, before (Cntl) and after treatment with NMDA, with and without MK801, CycA, or CycA+LY. Graphs display mean ± SEM (*n* = 100–200 spines from 7–10 cells per condition). Statistical analysis was performed using one-way ANOVA followed by Tukey's multiple-comparison posttest (*$P < 0.05$, **$P < 0.01$, ***$P < 0.001$).

be translocated to dendritic spines in its phosphorylated form, but fails to remodel spines (Fig. 5 *I–K*). These studies show that both calcineurin- and PI3K-mediated cofilin dephosphorylation and β-arrestin–mediated translocation of cofilin to dendritic spines are necessary for NMDA-mediated dendritic spine remodeling ([Fig. S2](#)).

Deletion of β-Arrestin-1, but Not β-Arrestin-2, Disrupts the Development of Mature Dendritic Spines in the Mouse Hippocampus in Vivo. We next examined whether development of mature dendritic spines is affected in the hippocampus of β-arrestin-1 KO and β-arrestin-2 KO mice in vivo. CA1 hippocampal neurons from β-arrestin-1 KO mice displayed longer spines with a significantly smaller head area and

lower head area-to-length ratio than did either WT or β-arrestin-2 KO neurons (Fig. 6 *A–F* and *I*). In contrast, β-arrestin-2 KO neurons developed normal mature dendritic spines, similar to those of WT neurons. There were no changes in the number of spines or percentage of filopodia among WT and β-arrestin KO neurons (Fig. 6 *G* and *H*). Whereas the development of mature dendritic spines is affected in β-arrestin-1 KO neurons, β-arrestin-2 KO neurons develop normal mature spines both in vitro and in vivo, but fail to remodel spines in response to NMDA-dependent chemical LTD in vitro.

β-Arrestin-2 KO Mice Exhibit Normal LTP, but Significantly Impaired LTD, in Acute Hippocampal Slices. The abnormal NMDA-mediated dendritic spine plasticity observed in the β-arrestin-2 KO neu-
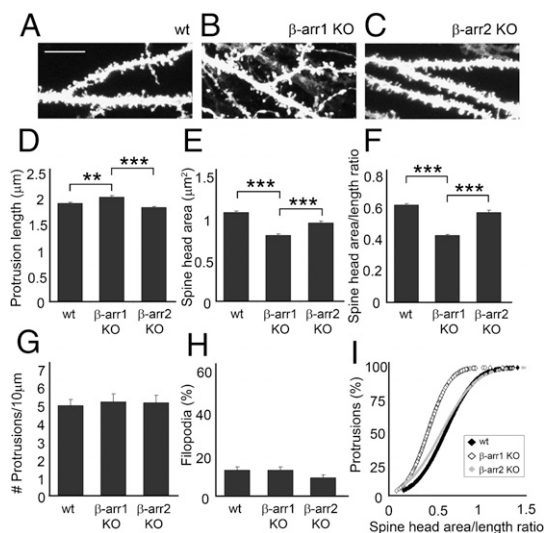
Fig. 6. Deletion of β-arrestin-1, but not β-arrestin-2, disrupts the development of mature dendritic spines in the mouse hippocampus in vivo. (A–C) Confocal images showing the dendrites of CA1 neurons labeled with 1,1′-dioctadecyl-3,3,3′,3′- tetramethylindocarbocyanine perchlorate (DiI) in hippocampal slices from WT, β-arrestin-1 KO, or β-arrestin-2 KO mice. (Scale bar, 10 μm.) (D–I) Quantitative analysis of the spine length (D), head area (E), head area/length ratio (F and I), number of protrusions per 10 μm of dendrite (G), and percentage of filopodia (H). Histograms show mean ± SEM (n = 700–800 spines from six to eight neurons per condition). Statistical analysis was performed using one-way ANOVA followed by Tukey's multiple-comparison posttest (**P < 0.01, ***P < 0.001).

rons in vitro suggested that deletion of β-arrestin-2 might result in altered synaptic plasticity. We induced LTP in acute hippocampal slices with two 1-s duration 100-Hz tetani of Schaffer collaterals (39). A potentiation of 150% of the field excitatory postsynaptic potentials (EPSPs) was found in both WT and β-arrestin-2 KO hippocampi following 60 min of high-frequency stimulation, suggesting that β-arrestin-2 KO mice exhibit normal levels of LTP (Fig. 7 A and B).

The cultured β-arrestin-2 KO neurons showed resistance to NMDA-induced spine head shrinkage, a mechanism that is associated with LTD, and Rust et al. (22) found significantly altered LTD in conditional cofilin KO mice. Therefore, we next induced LTD in Schaffer collateral-CA1 synapses using paired-pulse low-frequency stimulation (PP-LFS) at 1 Hz for 15 min. Interestingly, LTD was significantly impaired in β-arrestin-2 KO mice, as only a 1.2% depression was detected following 60 min of PP-LFS, compared with a 16.1% depression observed in WT mice (Fig. 7 C and D). In addition, EPSPs in the slices from the β-arrestin-2 KO mice returned to baseline 30 min after stimulation, whereas EPSPs in WT slices remained at 85% of baseline 60 min following stimulation. In contrast, there were no differences in input/output (I/O) curves between β-arrestin-2 KO and control mice (Fig. 7E), indicating that basal pre- and postsynaptic responses are not altered by knockout of β-arrestin-2. Taken together, these results implicate β-arrestin-2 in cellular mechanisms involving dendritic spine shrinkage and LTD.

β-Arrestin-2–Deficient Mice Display Deficits in Long-Term Spatial Learning. Resistance to NMDA-induced dendritic spine remodeling and impaired NMDA-dependent LTD suggested that hippocampal-dependent learning and memory may be also affected in the β-arrestin-2 KO mice. To examine the spatial learning abilities of β-arrestin-2 KO mice, we used the radial arm water maze, a highly sensitive test of hippocampal-dependent spatial memory (40, 41). Both WT and β-arrestin-2 KO mice performed similarly during days
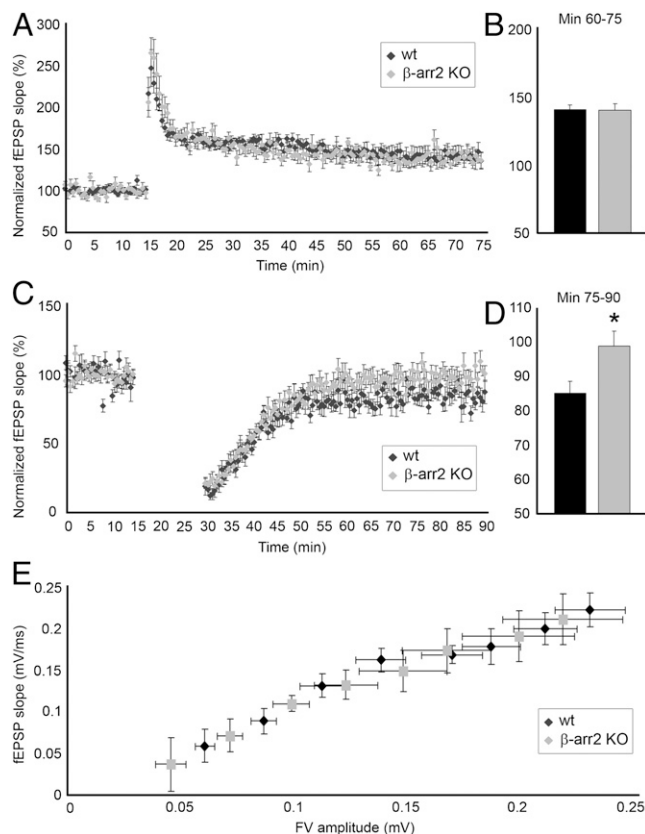

Fig. 7. β-Arrestin-2 KO mice exhibit normal LTP, but significantly impaired LTD, in acute hippocampal slices. (A) LTP of Schaffer collateral-CA1 synapses evoked by two trains of 100-Hz pulses at 1 s duration in WT (solid symbols) and β-arrestin-2 KO (shaded symbols) mice. Graph shows mean ± SEM (WT, n = 7; β-arrestin-2 KO, n = 7). (B) Quantitative analysis of extracellular field excitatory postsynaptic potentials (fEPSPs) for minutes 60–75 in WT (solid bar) and β-arrestin-2 KO (shaded bar) mice. Histogram shows mean ± SEM; Student's t test, not significant (NS). (C) LTD of Schaffer collateral-CA1 synapses evoked by paired-pulse LFS at 1 Hz for 15 min in WT (solid symbols) and β-arrestin-2 KO (shaded symbols) mice. Graph shows mean ± SEM (WT, n = 9; β-arrestin-2 KO, n = 10). (D) Quantitative analysis of fEPSPs for minutes 75–90 in WT (solid bar) and β-arrestin-2 KO (shaded bar) mice. Histogram shows mean ± SEM; Student's t test, *P = 0.027. (E) Input/output (I/O) curves as an indication of basal synaptic transmission for WT (solid symbols) and β-arrestin-2 KO (shaded symbols) mice. Graph shows mean ± SEM (WT, n = 17; β-arrestin-2 KO, n = 15); Student's t test, not significant (NS).

1–6 of the training, indicating that short-term reference memory was not altered in the β-arrestin-2 KO mice (Fig. 8). However, whereas WT mice continued to improve over the course of 11 d, β-arrestin-2 KO mice failed to show improvements from day 7 to day 11. β-Arrestin-2 KO mice needed significantly more time to locate the hidden platform at the end of the test on days 7–11 (Fig. 8 A, C, and E) and made significantly more errors in the process than did WT mice (Fig. 8 B, D, and F). These results reveal a deficit in long-term spatial learning and memory in the β-arrestin-2 KO mice.

β-Arrestin-2–Deficient Hippocampal Neurons Are Resistant to Aβ-Induced Dendritic Spine and Synapse Loss. The phospho-mimetic cofilin^{S3D} mutant was shown to be protective in hippocampal slices against spine loss induced by Aβ$_{1–42}$ oligomers that are implicated in Alzheimer's disease (AD) (26). In addition, the formation of Aβ-induced cofilin–actin rods in hippocampal slices and cultured neurons was prevented by enhancing cofilin phosphorylation through modulation of LIMK, slingshot phosphatase (SSH), and CIN (25). Here we have demonstrated that β-arrestin-2–deficient
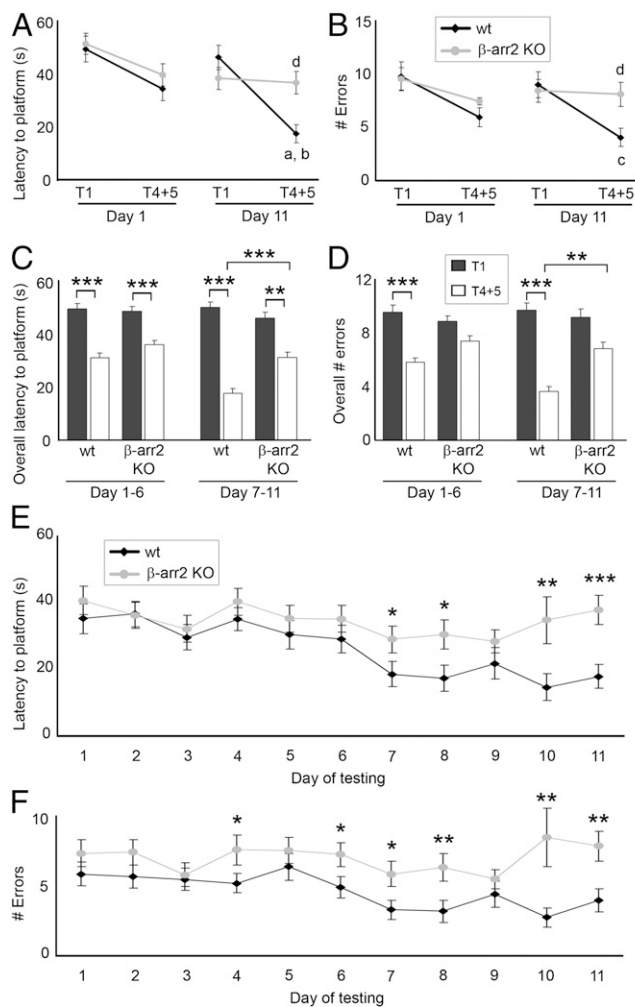
Fig. 8. β-Arrestin2–deficient mice display deficits in long-term spatial learning. (A–F) Quantitative analysis of the latency to locate the hidden platform (A, C, and E) and number of errors (B, D, and F) in the radial arm water maze over 11 d of testing. Graphs display mean ± SEM (WT, solid symbols, n = 13; β-arrestin-2 KO, shaded symbols, n = 12). (A and B) Statistical analysis was performed using one-way ANOVA followed by Tukey's multiple-comparison posttest. a, WT/D11/T4+5 shows significant improvement vs. WT/D1/T4+5 (P < 0.05); b and c, WT/D11/T4+5 shows significant improvement vs. WT/D11/T1 (b, P < 0.001; c, P < 0.05); d, β-arrestin-2 KO/D11/T4+5 is significantly impaired vs. WT/D11/T4+5 (P < 0.05). (B and D) Latency to find the platform (B) and number of errors (C) were averaged for the early days of testing (days 1–6) and the late days of testing (days 7–11) to evaluate long-term performance (**P < 0.01, ***P < 0.001). (E and F) Histograms show latency (E) and number of errors (F) for trials 4 and 5 (averaged). Statistical analysis for each individual day of testing was performed using Student's t test (*P < 0.05, **P < 0.01, ***P < 0.001).

neurons are resistant to NMDA-induced dendritic spine remodeling due to impaired spatial localization of cofilin in dendritic spines. We therefore tested whether depletion of β-arrestin-2 would also protect neurons against Aβ-mediated spine loss, similar to the effects of phospho-mimetic cofilin[S3D], which inhibits endogenous cofilin activity. Whereas Aβ promoted immature spines in WT neurons, β-arrestin-2–deficient neurons did not display spine remodeling with Aβ treatment (Fig. 9 A–I), and β-arrestin-2 deletion was also protective against spine loss induced by Aβ peptide (Fig. 9J). In addition, whereas Aβ induced a significant decrease in the overall numbers of synaptophysin-positive presynaptic terminals; postsynaptic sites containing PSD-95–, NR2A/B–, and GluR2-positive puncta; and phalloidin-positive F-actin

clusters in WT hippocampal neurons, β-arrestin-2–deficient neurons were resistant to these changes induced by Aβ treatment (Fig. 9 K–M). The numbers of the pre- and postsynaptic proteins that were associated with dendritic spines also did not change in Aβ-treated β-arrestin-2–deficient neurons (Fig. 9 N–P). These studies suggest that β-arrestin-2 may also be involved in some pathological forms of dendritic spine plasticity, such as Aβ-induced spine loss, and may emerge as a new target for AD therapies.

Discussion

Cofilin has recently been implicated as an important regulator of synaptic plasticity under both physiological and pathological conditions (20–22, 26, 42). Whereas active cofilin has been shown to preferentially associate with the more dynamic peripheral F-actin pool in dendritic spines (43), the phosphorylation of cofilin that suppresses its activity has been shown to promote mature stable mushroom-shaped spines in response to LTP (20). Furthermore, hippocampal neurons lacking cofilin exhibited an increased number of mushroom-shaped spines and showed a substantial enlargement of head area, indicating the prevalence of more mature spines (22). We have made similar observations, showing that the enhancement of cofilin activity by overexpression of constitutively active cofilin[S3A] leads to more immature spines and filopodia, whereas cofilin inhibition with phospho-mimetic cofilin[S3D] promotes stable mature mushroom spines (19). Temporal regulation of cofilin activity has also been implicated in AMPAR trafficking during synaptic potentiation and dendritic spine enlargement (42). Consistent with the structural role of cofilin in regulating spine morphology and AMPAR trafficking, cofilin was also shown to be involved in synaptic plasticity and learning (22, 42). Mice lacking cofilin have demonstrated impaired late LTP (L-LTP), LTD, and associative learning, including spatial learning, aversive learning, and reward learning (22). In addition, stress-induced cofilin–actin rods are found in the brain in several neurological disorders (24), and cofilin inhibition with phospho-mimetic cofilin[S3D] in hippocampal slices has been shown to prevent Aβ-mediated dendritic spine loss, which is a hallmark of AD (25, 26). It appears that temporal and spatial control over cofilin activity determines its effects on synapses. Here we report that the scaffolding protein β-arrestin-2 spatially regulates cofilin localization in synapses and plays an important role in NMDA-dependent dendritic spine/synapse plasticity, hippocampal LTD, and spatial learning.

β-Arrestins are known to be involved in the inactivation of G protein-coupled receptor (GPCR) signaling (27), but they are also recognized for their ability to regulate F-actin organization and cytoskeletal dynamics through the scaffolding of actin assembly proteins (30–32). β-Arrestins were recently shown to control the spatial localization of cofilin and its regulating proteins that act downstream of protease-activated receptor-2 (PAR-2) in fibroblasts and primary leukocytes (34, 44), and this process has been implicated in the formation of a leading edge and subsequent chemotaxis (34). Whereas β-arrestin-1 was shown to scaffold cofilin with LIMK, the kinase that phosphorylates and inactivates cofilin, β-arrestin-2 has been implicated in associating cofilin with the phosphatases CIN and SSH, leading to cofilin dephosphorylation and activation (33, 34, 44). The ability of β-arrestins to scaffold cofilin with its enzymes and to regulate dynamic changes in F-actin organization made it a prime candidate for the regulation of cofilin translocation into dendritic spines. Our data suggest that β-arrestin-1 is required for normal development of dendritic spines, as there is an increase in immature spines in the β-arrestin-1 KO hippocampal neurons under normal synaptic activity, both in vitro and in vivo. This result could be due to decreased association of LIMK with cofilin in β-arrestin-1–deficient mice, which could lead to increased cofilin activity. In addition, these neurons still express β-arrestin-2, which scaffolds cofilin with its activator SSH phosphatase, leading to a further increase in cofilin activation and
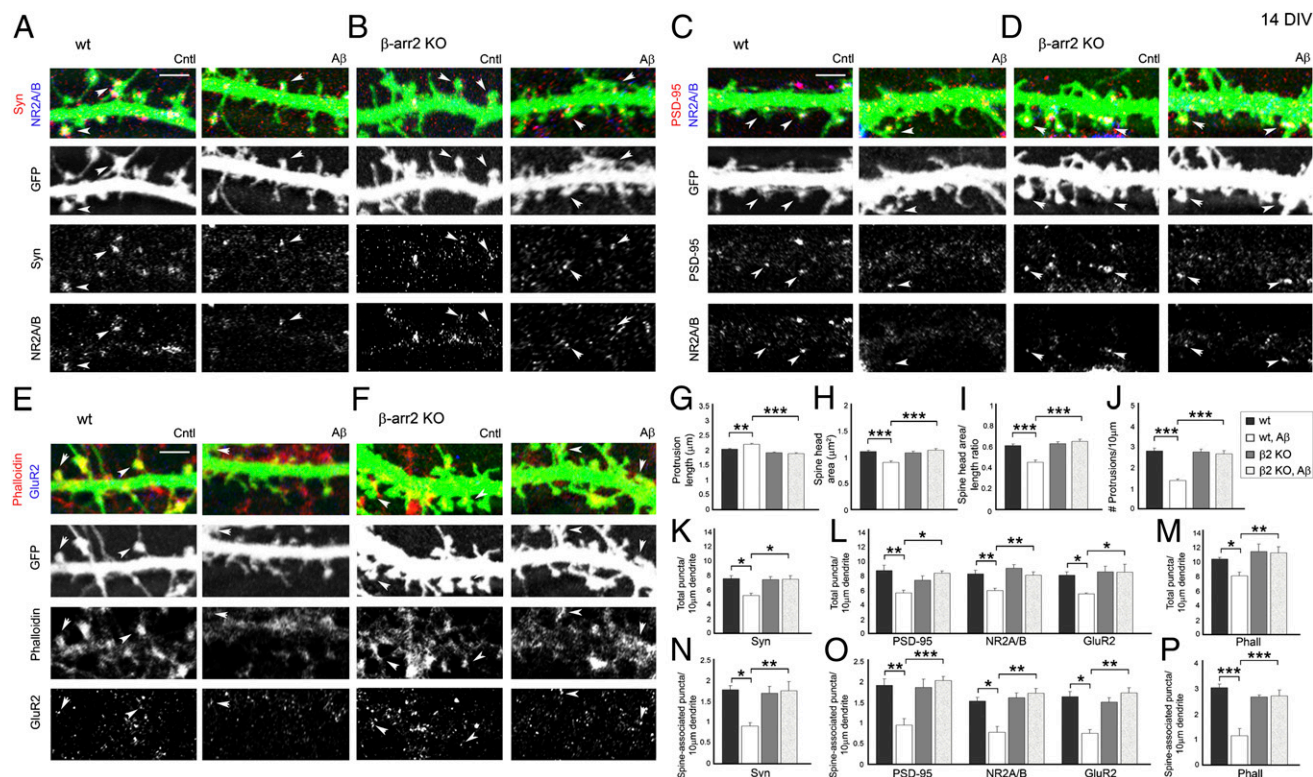
Fig. 9. β-Arrestin-2–deficient hippocampal neurons are resistant to Aβ-induced dendritic spine and synapse loss. (A–F) Confocal images showing GFP-expressing dendrites of 14 DIV hippocampal neurons from WT (A, C, and E) or β-arrestin-2 KO mice (B, D, and F), untreated (Cntl) or with application of 225 pM Aβ$_{1-42}$ oligomers for 24 h (Aβ). Pre- and postsynaptic sites were identified by immunostaining against synaptophysin (Syn, A and B), PSD-95 (C and D), the NMDAR subunits NR2A/B (A–D), and the AMPAR subunit GluR2 (E and F). F-actin was detected by rhodamine-coupled phalloidin (E and F). Arrowheads denote positive puncta that are associated with dendritic spines. (Scale bars, 10 μm.) (G–J) Quantitative analysis of spine length (G), head area (H), head area/length ratio (I), and density (J) in untreated or Aβ$_{1-42}$-treated (Aβ) neurons. Histograms show mean ± SEM (n = 7–10 neurons per condition). Statistical analysis was performed using one-way ANOVA followed by Tukey's multiple-comparison posttest (**P < 0.01, ***P < 0.001). (K–P) Quantitative analysis of the total number of synaptophysin (Syn-), PSD-95–, NR2A/B-, GluR2-, and Phalloidin (Phall)-positive puncta detected in both dendritic spines and shafts (K–M) or of the number of puncta associated with dendritic spines (N–P) per 10 μm in Aβ$_{1-42}$-treated (Aβ) WT or β-arrestin-2 KO neurons. Statistical analysis was performed using one-way ANOVA followed by Tukey's multiple-comparison posttest (*P < 0.05, **P < 0.01, ***P < 0.001).

affecting formation of mature dendritic spines. In support of this, overexpression of constitutively active cofilin[S3A] in β-arrestin-1 KO neurons leads to formation of cofilin–actin rods, structures formed under conditions of cellular stress when cofilin is excessively active (23, 35, 36, 45). In contrast, overexpression of phosphomimetic cofilin[S3D] restores mature dendritic spines in β-arrestin-1 KO neurons and prevents rod formation, most likely through competitive inhibition of cofilin dephosphorylation by SSH.

In contrast to the β-arrestin-1 KO neurons, dendritic spines in β-arrestin-2 KO neurons develop normally, but fail to remodel in response to NMDA-mediated chemical LTD. Our results show that deletion of β-arrestin-2 abolished the ability of NMDA or constitutively active cofilin[S3A] to induce spine head shrinkage and prevented a subsequent loss of synaptic proteins from dendritic spines. Although cofilin activation is required for NMDA-mediated remodeling of dendritic spines and synapses, dephosphorylation alone is not sufficient to trigger cofilin clustering in the spines. We see that inhibition of cofilin dephosphorylation by blocking calcineurin and PI3K does not inhibit NMDA-induced cofilin translocation, but does inhibit NMDA-induced spine remodeling, most likely because cofilin is phosphorylated and inactive. This result suggests that cofilin can be translocated to spines in response to NMDA independent of its dephosphorylation, which is mediated by calcineurin and PI3K. The mechanisms that accomplish spatial and temporal control over cofilin activity determine its synaptic effects, which can lead to spine shrinkage and LTD or spine enlargement and LTP. Our studies indicate that

β-arrestin-2 plays an important role in the regulation of cofilin localization in dendritic spines, which underlies NMDA-induced spine shrinkage and LTD. In fact, active cofilin failed to translocate into dendritic spines of β-arrestin-2 KO neurons following NMDA treatment, suggesting that β-arrestin-2 may regulate NMDA-mediated spine and synapse remodeling through cofilin translocation. In support of this, β-arrestin-2 KO neurons are also resistant to dendritic spine remodeling induced by constitutively active cofilin[S3A], which is aberrantly expressed in β-arrestin-2 KO neurons and fails to translocate to spines in response to NMDA. This result supports the role of β-arrestin-2 in both spatial localization of active cofilin and NMDA-induced dendritic spine remodeling, which are disrupted in β-arrestin-2 KO neurons and are recovered by overexpression of β-arrestin-2.

The ability of β-arrestin-2 to regulate cofilin localization may also underlie long-term synaptic plasticity and spatial learning, as β-arrestin-2–deficient mice exhibited deficits in the radial arm water maze and impaired NMDA-dependent hippocampal LTD, similar to effects observed by Rust et al. (22) in conditional cofilin KO mice. These studies suggest that the early phase of LTP is not dependent on changes in dendritic spine morphology and is therefore unaffected by the decrease in cofilin activity and the resulting decrease in spine plasticity in the β-arrestin-2 KO mice. Furthermore, it has recently been demonstrated that an LTP-blocking NMDAR 2A antagonist had no significant effect on spatial memory performance in a Morris water maze task in adult rats, whereas an LTD-blocking NMDAR 2B antagonist impaired spatial memory con-

solidation (46). These findings suggest that changes in LTD may underlie the impaired spatial learning in β-arrestin-2 KO mice.

In addition to mediating the dendritic spine plasticity that is thought to underlie normal learning and memory, β-arrestin-2 may also be involved in some pathological forms of spine remodeling. We show that whereas $A\beta_{1-42}$ oligomers induce loss of spines and synapses in WT hippocampal neurons, β-arrestin-2 deletion prevents spine and synapse loss, similar to the effects of phospho-mimetic cofilin[S3D] (26). It would be interesting to determine whether these events are also mediated through the NMDAR-dependent pathway or β-arrestin-2 acts through desensitization and internalization of G-protein–coupled receptors. Although the mechanism of β-arrestin-2 effects on Aβ-induced spine loss is still not clear, the involvement of β-arrestin-2 in some pathological forms of dendritic spine remodeling such as Aβ-induced spine loss could lead to a new target for AD therapies. Our studies implicate β-arrestin-2 in cofilin regulation during dendritic spine plasticity, hippocampal LTD, and spatial learning. We have shown here a unique function of β-arrestins that does not involve GPCR signaling, but regulates NMDA-mediated dendritic spine/synapse plasticity through the spatial control of cofilin activation.

Materials and Methods

Mice. β-Arrestin-1$^{-/-}$ and β-arrestin-2$^{-/-}$ mice on a C57BL/6 background were generous gifts from Robert Lefkowitz (Duke University Medical Center, Durham, NC). All experiments were conducted in accordance with National Institutes of Health guidelines for the care and use of animals with approval from the University of California, Riverside, Animal Care and Use Committee.

Expression Vectors. The expression vectors used were pEGFP-N1 and pDsRed-C2 (Clontech) and pcDNA3-EGFP-cofilin, pcDNA3-EGFP-cofilin^{S3A}, pcDNA3-EGFP-cofilin^{S3D}, pcDNA3-β-arrestin-1-FLAG, pcDNA3-β-arrestin-2-FLAG, and pGEX4T1-cofilin-GST (FLAG-tagged β-arrestin-1 and -2 plasmids were from Robert Lefkowitz).

Hippocampal Neuronal Cultures and Transfection. Cultures of hippocampal neurons were prepared from embryonic day 15 (E15) or E16 mice as previously described (18). The cultures were transfected at 12 DIV using the calcium phosphate method as previously described (18, 47). See *SI Materials and Methods* for more details on hippocampal neuronal cultures, biochemical analysis, immunocytochemistry, electrophysiology, behavioral testing, and microscopy.

1. Sorra KE, Harris KM (2000) Overview on the structure, composition, function, development, and plasticity of hippocampal dendritic spines. *Hippocampus* 10:501–511.
2. Hering H, Sheng M (2001) Dendritic spines: Structure, dynamics and regulation. *Nat Rev Neurosci* 2:880–888.
3. Rao A, Craig AM (2000) Signaling between the actin cytoskeleton and the postsynaptic density of dendritic spines. *Hippocampus* 10:527–541.
4. Ethell IM, Pasquale EB (2005) Molecular mechanisms of dendritic spine development and remodeling. *Prog Neurobiol* 75:161–205.
5. Matus A (2005) Growth of dendritic spines: A continuing story. *Curr Opin Neurobiol* 15:67–72.
6. Pontrello CG, Ethell IM (2009) Accelerators, brakes, and gears of actin dynamics in dendritic spines. *Open Neurosci J* 3:67–86.
7. Ashby MC, Maier SR, Nishimune A, Henley JM (2006) Lateral diffusion drives constitutive exchange of AMPA receptors at dendritic spines and is regulated by spine morphology. *J Neurosci* 26:7046–7055.
8. Matsuzaki M, et al. (2001) Dendritic spine geometry is critical for AMPA receptor expression in hippocampal CA1 pyramidal neurons. *Nat Neurosci* 4:1086–1092.
9. Yuste R, Bonhoeffer T (2001) Morphological changes in dendritic spines associated with long-term synaptic plasticity. *Annu Rev Neurosci* 24:1071–1089.
10. Halpain S, Spencer K, Graber S (2005) Dynamics and pathology of dendritic spines. *Prog Brain Res* 147:29–37.
11. Penzes P, Cahill ME, Jones KA, VanLeeuwen JE, Woolfrey KM (2011) Dendritic spine pathology in neuropsychiatric disorders. *Nat Neurosci* 14:285–293.
12. Moriyama K, Matsumoto S, Nishida E, Sakai H, Yahara I (1990) Nucleotide sequence of mouse cofilin cDNA. *Nucleic Acids Res* 18:3053.
13. Yahara I, et al. (1996) A role of cofilin/destrin in reorganization of actin cytoskeleton in response to stresses and cell stimuli. *Cell Struct Funct* 21:421–424.
14. Carlier MF, et al. (1997) Actin depolymerizing factor (ADF/cofilin) enhances the rate of filament turnover: Implication in actin-based motility. *J Cell Biol* 136:1307–1322.
15. Lappalainen P, Drubin DG (1997) Cofilin promotes rapid actin filament turnover in vivo. *Nature* 388:78–82.
16. Rosenblatt J, Agnew BJ, Abe H, Bamburg JR, Mitchison TJ (1997) Xenopus actin depolymerizing factor/cofilin (XAC) is responsible for the turnover of actin filaments in Listeria monocytogenes tails. *J Cell Biol* 136:1323–1332.
17. Bamburg JR (1999) Proteins of the ADF/cofilin family: Essential regulators of actin dynamics. *Annu Rev Cell Dev Biol* 15:185–230.
18. Shi Y, Ethell IM (2006) Integrins control dendritic spine plasticity in hippocampal neurons through NMDA receptor and Ca2+/calmodulin-dependent protein kinase II-mediated actin reorganization. *J Neurosci* 26:1813–1822.
19. Shi Y, Pontrello CG, DeFea KA, Reichardt LF, Ethell IM (2009) Focal adhesion kinase acts downstream of EphB receptors to maintain mature dendritic spines by regulating cofilin activity. *J Neurosci* 29:8129–8142.
20. Chen LY, Rex CS, Casale MS, Gall CM, Lynch G (2007) Changes in synaptic morphology accompany actin signaling during LTP. *J Neurosci* 27:5363–5372.
21. Zhou Q, Homma KJ, Poo MM (2004) Shrinkage of dendritic spines associated with long-term depression of hippocampal synapses. *Neuron* 44:749–757.
22. Rust MB, et al. (2010) Learning, AMPA receptor mobility and synaptic plasticity depend on n-cofilin-mediated actin dynamics. *EMBO J* 29:1889–1902.
23. Davis RC, et al. (2009) Mapping cofilin-actin rods in stressed hippocampal slices and the role of cdc42 in amyloid-beta-induced rods. *J Alzheimers Dis* 18:35–50.
24. Maloney MT, Bamburg JR (2007) Cofilin-mediated neurodegeneration in Alzheimer's disease and other amyloidopathies. *Mol Neurobiol* 35:21–44.
25. Davis RC, et al. (2011) Amyloid beta dimers/trimers potently induce cofilin-actin rods that are inhibited by maintaining cofilin-phosphorylation. *Mol Neurodegener* 6:10.
26. Shankar GM, et al. (2007) Natural oligomers of the Alzheimer amyloid-beta protein induce reversible synapse loss by modulating an NMDA-type glutamate receptor-dependent signaling pathway. *J Neurosci* 27:2866–2875.
27. Luttrell LM, Lefkowitz RJ (2002) The role of beta-arrestins in the termination and transduction of G-protein-coupled receptor signals. *J Cell Sci* 115:455–465.
28. Defea K (2008) Beta-arrestins and heterotrimeric G-proteins: Collaborators and competitors in signal transduction. *Br J Pharmacol* 153(Suppl 1):S298–S309.
29. DeWire SM, Ahn S, Lefkowitz RJ, Shenoy SK (2007) Beta-arrestins and cell signaling. *Annu Rev Physiol* 69:483–510.
30. Wang P, DeFea KA (2006) Protease-activated receptor-2 simultaneously directs beta-arrestin-1-dependent inhibition and Galphaq-dependent activation of phosphatidyl-inositol 3-kinase. *Biochemistry* 45:9374–9385.
31. Bhattacharya M, et al. (2002) Beta-arrestins regulate a Ral-GDS Ral effector pathway that mediates cytoskeletal reorganization. *Nat Cell Biol* 4:547–555.
32. Barlic J, et al. (2000) Regulation of tyrosine kinase activation and granule release through beta-arrestin by CXCRI. *Nat Immunol* 1:227–233.
33. Xiao K, et al. (2010) Global phosphorylation analysis of beta-arrestin-mediated signaling downstream of a seven transmembrane receptor (7TMR). *Proc Natl Acad Sci USA* 107:15299–15304.
34. Zoudilova M, et al. (2010) beta-Arrestins scaffold cofilin with chronophin to direct localized actin filament severing and membrane protrusions downstream of protease-activated receptor-2. *J Biol Chem* 285:14318–14329.
35. Bamburg JR, et al. (2010) ADF/Cofilin-actin rods in neurodegenerative diseases. *Curr Alzheimer Res* 7:241–250.
36. Minamide LS, Striegl AM, Boyle JA, Meberg PJ, Bamburg JR (2000) Neurodegenerative stimuli induce persistent ADF/cofilin-actin rods that disrupt distal neurite function. *Nat Cell Biol* 2:628–636.
37. Wang Y, Shibasaki F, Mizuno K (2005) Calcium signal-induced cofilin dephosphorylation is mediated by Slingshot via calcineurin. *J Biol Chem* 280:12683–12689.
38. Carlisle HJ, Manzerra P, Marcora E, Kennedy MB (2008) SynGAP regulates steady-state and activity-dependent phosphorylation of cofilin. *J Neurosci* 28:13673–13683.
39. Agulhon C, Fiacco TA, McCarthy KD (2010) Hippocampal short- and long-term plasticity are not modulated by astrocyte Ca2+ signaling. *Science* 327:1250–1254.
40. Arendash GW, et al. (2006) Caffeine protects Alzheimer's mice against cognitive impairment and reduces brain beta-amyloid production. *Neuroscience* 142:941–952.
41. Cao C, et al. (2009) Abeta-specific Th2 cells provide cognitive and pathological benefits to Alzheimer's mice without infiltrating the CNS. *Neurobiol Dis* 34:63–70.
42. Gu J, et al. (2010) ADF/cofilin-mediated actin dynamics regulate AMPA receptor trafficking during synaptic plasticity. *Nat Neurosci* 13:1208–1215.
43. Racz B, Weinberg RJ (2006) Spatial organization of cofilin in dendritic spines. *Neuroscience* 138:447–456.
44. Zoudilova M, et al. (2007) Beta-arrestin-dependent regulation of the cofilin pathway downstream of protease-activated receptor-2. *J Biol Chem* 282:20634–20646.
45. Minamide LS, et al. (2010) Isolation and characterization of cytoplasmic cofilin-actin rods. *J Biol Chem* 285:5450–5460.
46. Ge Y, et al. (2010) Hippocampal long-term depression is required for the consolidation of spatial memory. *Proc Natl Acad Sci USA* 107:16697–16702.
47. Jiang M, Chen G (2006) High Ca2+-phosphate transfection efficiency in low-density neuronal cultures. *Nat Protoc* 1:695–700.